Assessing the use of digital imaging to estimate the growth performance of young cassava

Yaw Ohene Afrane
Master's thesis
MSc. Environment and Natural Resources
University of Helsinki
Department of Agricultural Sciences
October 2020

HELSINGIN YLIOPISTO — HELSINGFORS UNIVERSITET — UNIVERSITY OF HELSINKI

Tiedekunta/Osasto — Fakultet/Sektion — Faculty	Laitos — Institution — Department
Faculty of Agriculture and Forestry	Department of Agricultural Science

Tekijä — Författare — Author

Yaw Ohene Afrane

Työn nimi — Arbetets titel — Title

Assessing the use of digital imaging to estimate the growth performance of young cassava

Oppiaine —Läroämne — Subject

Agrotechnology

Työn laji — Arbetets art — Level	Aika — Datum — Month and year	Sivumäärä — Sidoantal — Number of pages
Master's thesis	October 2020	41

Tiivistelmä — Referat — Abstract

The world population is growing and is expected to reach over 9 billion in about 30 years. Climate change is also widely expected to worsen famines in certain regions of the world. This will drastically increase global food demand. Food security efforts should be therefore be geared towards promoting food crops that can thrive in these regions and can withstand the condition likely to be brought about by changing climate. Cassava is a typical example of such a crop. This study investigated the use of digital images to estimate growth parameters of young cassava plants. Cassava was cultivated in pots at the University of Helsinki greenhouse at Viikki. The plants were given different water level (100%, 60% and 30% saturation) and potassium (0.1, 1.0, 4.0, 16.0 and 32.0mM) treatments. Digital red-green-blue (RGB) and multispectral images were taken every other week for 5 consecutive times. The images were processed to obtain leaf area, Normalized Difference Vegetation Index (NDVI), and Crop Senescence Index (CSI) and correlated with directly measured growth parameters of the young cassava crops. It was observed that leaf area that was computed from images, and NDVI which was computed from the multispectral images have significant positive correlations with the growth parameters, ie, actual leaf area, chlorophyll content, and plant biomass. CSI however showed weak a correlation between the growth parameters of the young cassava plants. Images leaf area and NDVI were then used to identify the changes in the effects of the water and potassium treatments.

Avainsanat — Nyckelord — Keywords

Imaging, NDVI, cassava, RGB, biomass, leaf area, multispectral

Säilytyspaikka — Förvaringsställe — Where deposited

Department of Agricultural Sciences and Viikki Campus Library

Muita tietoja — Övriga uppgifter — Further information

Contents

List of abbreviations

CRP: Calibration reflectance Panel

CSI: Crop Senescence Index

DAP: Days after planting

GA: Green area

GGA: Greener area

LAI: Leaf area index

NDVI: Normalized Difference vegetation index

NIR: Near-infrared

RGB: Red green blue

RH: Relative humidity

SIFT: Scale-invariant feature transform

UAV: Unmanned aerial vehicle

GNDVI: Green normalized difference vegetation index

GRVI: Green red vegetation index

MTCI: MERIS terrestrial chlorophyll index

SAVI: Soil adjusted vegetation index

EVI: Enhanced vegetation index

NPCI: Normalized pigment chlorophyll ratio index

CI: Chlorophyll index

PSRI: Plant Senescence Reflectance Index

1. Introduction

The world population is expected to grow up to 9.6 billion people by 2050 (Gerland et al, 2014). The population of sub-Saharan Africa alone is estimated to double between 2019 and 2050 (UN DESA, 2019) and food demand may not improve substantially between the period of 2010 and 2050 (Keating et al, 2014). Therefore, more effort must be put into research into finding better ways to improve food production, especially in developing regions where the population relies on indigenous food crops like cassava (*Manihot esculenta* Crantz). There is the need to encourage local people in places that are vulnerable or susceptible to food insecurity to cultivate and rely on indigenous crops that are resilient in their climate and can withstand harsh conditions that climate change may bring about. One such crop is cassava. Cassava is a common food that is consumed by half a billion people in and around the tropical region of Africa, Latin America (Mabrouk, 2003). Both leaves and root tubers of cassava are consumed as food (Lancaster and Brooks, 1983). A model on the consequence of climate on some tropical food crops showed that unlike crops like banana (*Musa acuminata colla*), cowpea (*Vigna unguiculata*), *Sorghum*, and potato (*Solanum tuberosum*) production which are likely to be negatively impacted by the effects of climate change in the year 2030, cassava showed very strong resilience and even could have a positive effect in some cases (Jarvis et al, 2012). Studies must therefore be conducted to identify optimum conditions for cassava production and to ascertain the effect of various soil nutrient levels on the crop.

For farmers, especially those in developing countries, to maximize food production they should be able to easily determine the health and optimum condition of the crop in a way that is not expensive at any time throughout the planting period. The use of normal colored/RGB (red-green-blue) images (RGB camera images) can be a cheap way to analyze the plant conditions (Cambaza et al, 2019).

Considerable work has been done on using imaging tools to crop science but very little has focused on cassava (Okogbenin et al, 2013). The overall aim is to study the effects of potassium fertilization and irrigation level on cassava growth and yield, as well as nutritive traits responses. The present study focuses on the use of imaging techniques to gather important data on cassava. It further contributes to earlier research findings on cassava published by Wasonga et al. (2020).

2. Literature Review

2.1. Need for imaging in crop production

Phenotyping helps in identifying desirable characteristics for plant breeding and crop management (Ghanem et al, 2015). Traditional methods of determining plant characteristics like biomass usually involve cutting samples to weigh and dry (Samuelsson et al, 2006). These methods are destructive and hence can be done mostly only at harvest time. This reduces the timeliness and quantum of work that can be done (Araus et al, 2018). The use of imaging techniques can provide an avenue to study some characteristics and the effects of certain treatment in a non-destructive way that can also be scaled up to various levels (Cardim Ferreira Lima et al, 2020), hence can do at any stage of growth.

2.2. Remote Sensing

Remote sensing is the acquisition of information from a subject through data without being in contact with the subject (Lillesand 2012, Kiefer et al. 2015). Therefore, the most basic form of remote sensing is a visual observation with the eye. Data that can be remotely sensed include acoustic waves like sonar, force distribution like gravitational or magnetic forces, and electromagnetic energy like visible light and radio waves (Lillesand et al. 2015). For this study, the focus is on the use of imaging hence the collection of electromagnetic energy data.

Using imaging in phenotyping and characteristic identification of plants involves the interaction of the substances that make up the plant and light energy, for example, blue and red light mostly absorbed by chlorophyll and green light is reflected by it (Li et al. 2014). Data on the different levels of reflectance of a subject in the various wavelengths of the electromagnetic spectrum is known as its reflectance signature/spectra. An example of a chart that shows the reflectance signature of some subjects is shown in Figure 1.

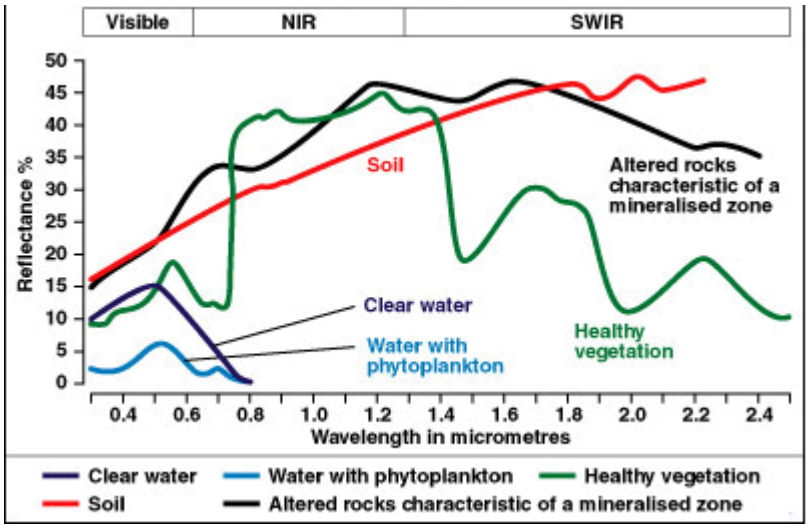

Figure 1. Generalized reflectance spectra/signature of various surfaces. NIR = Near-infrared SWIR=Short-wave infrared. (source: https://www.usna.edu/Users/oceano/pguth/md_help/html/ref_spectra.htm)

Usually, remote sensing is executed by passively capturing reflectance data of solar radiation that hits the subject (Aggarwal 2004) to get the portion that is reflected or absorbed. But some sensors can measure the energy that is emitted by the subjects themselves, like heat from the earth itself, while other sensors actively emit the energy themselves and read the reflection that is bounced back from the subject (Kerle et al. 2004).

2.3. RGB Imaging

A red-green-blue (RGB) image is a two-dimensional array of color pixels with each pixel corresponding to red (625–740 nm), green (500–565 nm), and blue (450–485 nm) components at a specific intensity (Alsultanny, 2010). RGB imaging has been used in the fields of agriculture, medicine, biology, etc. Formally, the agricultural application of imaging techniques was confined to images captured by techniques of remote sensing using satellites and/or aircraft and then processed and analyzed using computers. However, advancement in image capture and data processing have brought significant contributions to the advancement of different plant phenotyping aspects and hence provided solutions to various practical problems through the use of imaging techniques such as photometric feature-based imaging, fluorescence imaging, thermal imaging, and hyper-spectral imaging (Gupta et al., 2014; Cambaza et al., 2019). RGB imaging

which is a photometric feature-based technique has been used in recent times due to its dependency on the color variation of different biological samples, which replaced the human vision system. It is an affordable approach for analysis (Araus et al., 2018) compared to other approaches.

2.4. Multispectral Imaging and Image Analysis

Multispectral imaging is the process used to observe an object by the use of selected ranges of wavelengths in the electromagnetic spectrum that includes and extends beyond the capabilities of the human eye (Dyer et al. 2013). This process requires the use of multispectral cameras that have sensors to capture images in the different ranges of the wavelength of the electromagnetic spectrum, also known as bands, some of which are documented in Table 1. Some of the bands of wavelengths that are usually used in multispectral imaging are x-ray (0.01−10nm), ultraviolet (10−400nm), visible light (400−700nm), near-infrared (700−3000nm), mid-infrared (3000−7000nm), and thermal infrared (7000−3x10^5nm) (Norgard 2017).

Multispectral imaging techniques can equip us with the ability to determine some physical properties like biomass, canopy cover, and leaf area index, as well as chemical properties of green vegetation like chlorophyll, nitrogen, cellulose, water, phosphorous, protein, amino acids, sugar, and starch (Pullanagari et al. 2012, Gao et al. 2013 and Curran et al. 2001). Multispectral data is collected and compiled in the different bands of the electromagnetic spectrum and used to compute for various vegetation indexes, which are then used to predict physiological and agronomic traits performance of the plant (Gizaw et al. 2016). Some of these vegetation indexes are stated in Table 2.

Table 1: Some commonly used multispectral cameras

Sensor	Image	Bands	Source
Sentera quad		1 RGB 3 monochromes (635−675nm 710−740nm 785−815nm)	Sentera Inc, 2017
Tetracam ADC micro		Green Red Near-infrared	Tetracam Inc, 2017
Buzzard Six Band Multispectral Camera	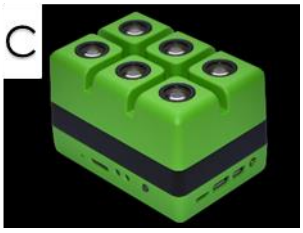	1 Blue 1 Green 1 Red 3 Red edge (704 nm, 740 nm, and 782 nm)	Buzzard Cameras Limited, 2018.
Parrot Sequoia		Green Red Red edge Near-infrared	Parrot drones SAS, 2017.
MicaSense Red edge		Green Blue Red Near-Infrared Red Edge	MicaSense Inc, 2015

Table 2: Some common vegetation indexes. (R = the reflectance in the specified band).

Vegetation Index	Formulae	Reference
Simple ratio	$\frac{R_{NIR}}{R_{red}}$	Jordan, 1969
Normalized difference vegetation index (NDVI)	$\frac{R_{NIR} - R_{red}}{R_{NIR} + R_{red}}$	Deering, 1978
Green normalized difference vegetation index (GNDVI)	$\frac{R_{NIR} - R_{green}}{R_{NIR} + R_{green}}$	Gitelson and Merzlak, 1996
Green red vegetation index (GRVI)	$\frac{R_{green} - R_{red}}{R_{green} + R_{red}}$	Tucker 1979
MERIS terrestrial chlorophyll index (MTCI)	$\frac{R_{NIR} - R_{rededge}}{R_{rededge} + R_{red}}$	Dash and Curran, 2004
Soil adjusted vegetation index (SAVI)	$\frac{(R_{NIR} - R_{red})(1 + L)}{R_{NIR} + R_{red} + L}$ L = adjusted parameter	Huete, 1988
Enhanced vegetation index (EVI)	$\frac{2.5(R_{NIR} - R_{red})}{R_{NIR} + 6R_{red} - 7.5R_{blue} + 1}$	Huete et al., 2002
Normalized pigment chlorophyll ratio index (NPCI)	$\frac{R_{red} - R_{blue}}{R_{red} + R_{blue}}$	Merzlyak et al., 1999
Chlorophyll index (green) (CI_{green})	$\frac{R_{NIR}}{R_{green}} - 1$	Gitelson, 2003
Chlorophyll index (red edge) (CI_{green})	$\frac{R_{NIR}}{R_{red\ edge}} - 1$	Gitelson, 2003
Plant Senescence Reflectance Index (PSRI)	$\frac{R_{red} - R_{green}}{R_{NIR}}$	Lee, 2008

2.5. Biomass Estimation

The accumulation of biomass is a key trait in ecological practices, plant breeding, and agricultural improvement. It is a crucial indicator of the performance of the plant as well as the final product of the crop (Chen et al. 2018). Typically, the measurement of plant biomass is destructive, time-

consuming, labor-intensive, and cannot be studied over time. Crop monitoring using non-destructive monitoring is however very important for agronomy and crop breeding (Brocks et al. 2018).

Remote sensing (digital image analysis) has therefore been adopted as a non-destructive method for estimations in various fields due to advancement in technology (Pullanagari et al. 2012, Easlon and Bloom 2014, Kefauver et al., 2017, Brocks et al 2018, Chen et al. 2018, Cambaza et al, 2019). Table 3 presents a compilation of some results of the use of imaging in biomass estimation.

Table 3: Results from literature that shows the use of imaging in biomass estimation.

Remarks	Source
Normalized Difference Vegetation Index, Optimized Soil-Adjusted Vegetation Index, simple ratio, Green Red Vegetation Index, and Modified Simple Ratio show small differences in the effects of different treatment	Cardim Ferreira Lima et al (2020)
Crop surface model was able to predict plant heights using RGB images. They then used the plant height to estimate crop biomass with 61–72% accuracy of fresh and 39–68% of dry barley (*Horedeum vulgare*).	Bendig et al. (2014)
By applying a backscattering coefficient scale, better correlation of Ratio Vegetation Index (RVI), the Normalized Difference Vegetation Index (NDVI), and the Enhanced Vegetation Index (EVI)	Gao et al. 2013

2.6. Leaf Area Estimation

Estimating leaf area in a non-destructive, accurate, and rapid way is essential for plant physiological and ecological assessments (Easlon and Bloom, 2014). The older methods where the obstruction of light was used have been replaced by digital technology (cameras, scanners, image processing, etc). ImageJ and Easy Leaf Area are software developed to estimate leaf area (Rasband 1997, Easlon and Bloom 2014). Both software have their pros and cons and have been used by several researchers. Whereas the ImageJ software, which is the commonest used, makes use of a threshold-based pixel count (Gracia-Romero et al. 2017) the Easy leaf Area software combines thresholding, component analysis, and color ratios to estimate leaf area (Easlon et al. 2014).

The orientation of leaves is important in leaf area measurements. Measuring the area of detached leaves can give a better estimate of the total leaf while capturing the area of leaves that are attached to the plant in their natural orientation creates a silhouette that has some of the leaves hidden behind

others (Smith, 1991). A compilation of some results of studies on leaf area estimation is presented in Table 4.

Easy Leaf Area takes a few seconds to process individual images or several minutes to batch process hundreds of images to measure leaf area. The software was written in python and the output is stored in both spreadsheet-ready CSV files and lossless TIFF files (Easlon and Bloom, 2014).

Table 4: Some results on literature on leaf area estimation.

Remarks	Source
When leaf length and width of Niagara and DeChaunac grapevines were correlated with a computerized image processing system, a regression of above $R^2 = 0.90$ was obtained. These single variable exponential models were generated: Area $=0.637W^{1.995}$, R^2=0.9821, and S.E.=10.58 for Niagara; and: area$=0.672W^{1.963}$, R2=0.9632, S.E.=5.67 for DeChaunac.	Williams III, Martinson 2003
In a study that assessed factors that affect the accuracy of using 3D lidar to estimate the leaf area density, the following factors were found to make the most effects: • Presence of non-photosynthetic tissues • The mean projection of a unit leaf area on a plane perpendicular to the direction of the laser beam • Number of incident laser beams in each region within the canopy • Distribution of leaf inclination angles Non-photosynthetic tissues and leaf inclination angle affected the leaf area estimate by 4.2–32.7% and 7.2–94.2%, respectively.	Hosoi 2007
In a study where the use of Photoshop CS6 was assessed to determine leaf areas of local grapes, it was observed that the pixel values were able to estimate leaf area with an accuracy of about 99.96– 100.00%.	Dogan et al. 2018

3. Objectives:

The main objective of this study was to assess the usage of imaging in cassava production. In the experiment, the specific objectives are to:

1. study the correlations between directly measured data and data obtained from images.
2. ascertain if the data that was obtained from the images would be able to identify the differences in the effects of water and potassium deficit on the young cassava plants.

4. Material and methods

4.1. Experimental setup planting material

The experiment was conducted in the greenhouse of the Viikki Plant Growth Facility of the University of Helsinki between January and November of 2018. It involved 3 indoor experiments using yellow cassava genotype "Mutura" (Kenya Agricultural and Livestock Research Organization (KALRO)). The growth conditions were set to day/night temperature of 27/17 °C, 55% RH, 600 μmol m^{-2} s^{-1} photosynthetic photon flux density, and 12 hours day length which were maintained throughout the experiment.

The experiment was set up as described by (Wasonga et. al. 2020). Cassava stem cuttings were grown in 5-liter pots and uniformly water for 30 days, after which there were randomly divided into three watering levels: full (100%), mild stress (60%), and severe stress (30%). Each irrigations treatment was further divided into 0.01mM, 1mM, 4mM, 16mM and 32 mM potassium (K) treatments. The different watering and K treatments were continually done every other day until 90 days after planting (DAP). The treatment combinations had 4 replicates each in a complete randomized block design as shown in Figure 2.

4.2. Image data collection

Figure 2. Photo that shows how the pots of cassava plants were setup in the greenhouse during the growing period.

Figure 3. Multispectral camera being used to capture data in the greenhouse. The camera was connected to a drone for power and hang to the roof of the greenhouse by cables to capture the pot of cassava on the bench.

RGB and multispectral image data were collected every fortnight (30, 45, 60, 75, and 90 DAP) during the treatment phase of the experiment. Every pot of cassava for all the treatments was captured. RGB data was captured with a Canon EOS 760D digital camera (Canon Inc, Ōta, Tokyo, Japan), shown in Figure 4, of the side view of the crops. The technical specifications of the camera are in Table 5. The RGB images were saved as JPEG files. The camera was placed at 1.4 m away from the plants. Two side-images of each plant was captured by rotating the plants 90 degrees after the first image capture. Multispectral data was captured with a MicaSense RedEdge™ 3 Multispectral Camera (MicaSense Inc, Seattle, WA, USA), as seen in Table 1 image E, of the top view from 1.6 m from the base of the pots. The multispectral camera captured data in the following bands: blue (465−485 nm), green (550−570 nm), red (663−673 nm), near-infrared (820—860 nm), and red edge (712−723 nm). Multispectral images were saved in a monochromatic TIFF file format (Figure 6). All images were captured during clear days and greenhouse lights were switched off during those moments. The MicaSense multispectral camera was calibrated using the MicaSense calibrated reflectance panel (CRP). The reflectance of the various bands is computed by dividing the average reflectance from the CRP image by the average radiance from pixel values from the image being processed (MicaSense, 2019).

Figure 4. Canon EOS 760D digital camera
(https://www.amateurphotographer.co.uk/reviews/dslrs/canon-eos-760d-review)

Table 5. Technical specification of the RGB camera.

Brand	Canon
Model	EOS 760D
Effective pixels	24.2 megapixels
Sensor size:	22.3 x 14.9 mm
Max. image resolution:	6000 x 4000
ISO:	Auto, 100 - 12800
Max. shutter speed:	1/4000 sec

4.3. Image processing

4.3.1. Red-Green-Blue Images Processing

The RGB images were analyzed with Easy leaf area (Ealson, 2014) to determine the leaf area. It is a free-to-use opensource software (Easlon, 2014). It was used to calculate the leaf area from RGB images regardless of the camera distance. To compute the area of green leaves in an image, a red flat object, like a colored sheet of paper, with a known surface area was placed next to the plant as a calibration sheet. The software processes and distinguishes between the red pixels from the calibration sheet and the green pixels from the leaves. The green pixels in the image are taken as leaves (Figure 5). Caution was taken to ensure that the background of the image contains no other red or green objects lest it be taken as calibration or leaves which will reduce the accuracy of the results. The software can automatically set an appropriate threshold for greenness to be able to capture all the green leaves in the picture but in instances where not all the leaves are captured, there are color threshold sliders to adjust the thresholds. The total leaf area is calculated with the equation

$$\text{total leaf area} = \frac{\text{green pixels}}{\text{red pixels}} \times \text{area of red calibration} \quad \textbf{(1)}$$

Figure 5. The normal RGB photo (A) and the green area identified by the Easy Leaf Area software (B).

Breedpix of the CIMMYT maize scanner plugin in Fiji ImageJ opensource software (Abràmoff et al. 2004) was used to analyze the characteristics of color to get RGB indices of the crops (Kefauver et al. 2017). The important indices that were collected are Green Area (GA) which is the fraction of the greenish pixels in the image; Greener Area (GGA) which is the fraction of deep green pixels in the image (Casadesús et al., 2007). This is then used to compute the Crop Senescence Index (CSI). The CSI gives a measure of active or healthy leaves in the images (ZamanAllah et al., 2015). Also, hue, saturation, and intensity were extracted from the RGB images using Breedpix (Casadesús et al., 2007). Saturation describes how pure the colors of an image are concerning greyness; hue refers to the average wavelength of light which is dominant, and intensity specifies how bright a color is (Carper et al. 1990).

$$CSI = 100 * \left(\frac{GA - GGA}{GA}\right) \qquad (2)$$

4.3.2. Multispectral image processing

The multispectral images were used to determine the Normalized Difference Vegetation Index (NDVI) of the crops. NDVI was chosen because is the most commonly used vegetation index (Jiang et al. 2006) hence a good starting point for studying the use of imaging tools for cassava production. The NDVI's were computed using the following equation

$$NDVI = \frac{R_{NIR} - R_{red}}{R_{NIR} + R_{red}} \quad (3)$$

Where R_{NIR} is the average reflectance in the near-infrared band and R_{red} is average reflectance in the red portion of visible light of the electromagnetic spectrum (Carlson and Ripley, 1997). The images from the various bands as captured by the MicaSense multispectral camera were not perfectly aligned because the various lenses are not coaxial, instead, they are placed apart from each other. This creates images that are captured from angles and hence merging them showed a misalignment distortion. The Scale-invariant feature transform (SIFT) algorithm (Lindeberg 2012) was used to correct the misalignment of the images (Figure 7). The SIFT algorithm uses feature recognition to identify corresponding points in multiple images for various processing like aligning, merging, and creating mosaics (Lindeberg, 2012). Also, Fiji Image J software was used for processing the multispectral images. The image calculator tool in ImageJ was used to compute the NDVIs (Figure 8). And a threshold was used to mark out the area covered by only the cassava plant (Figure 9).

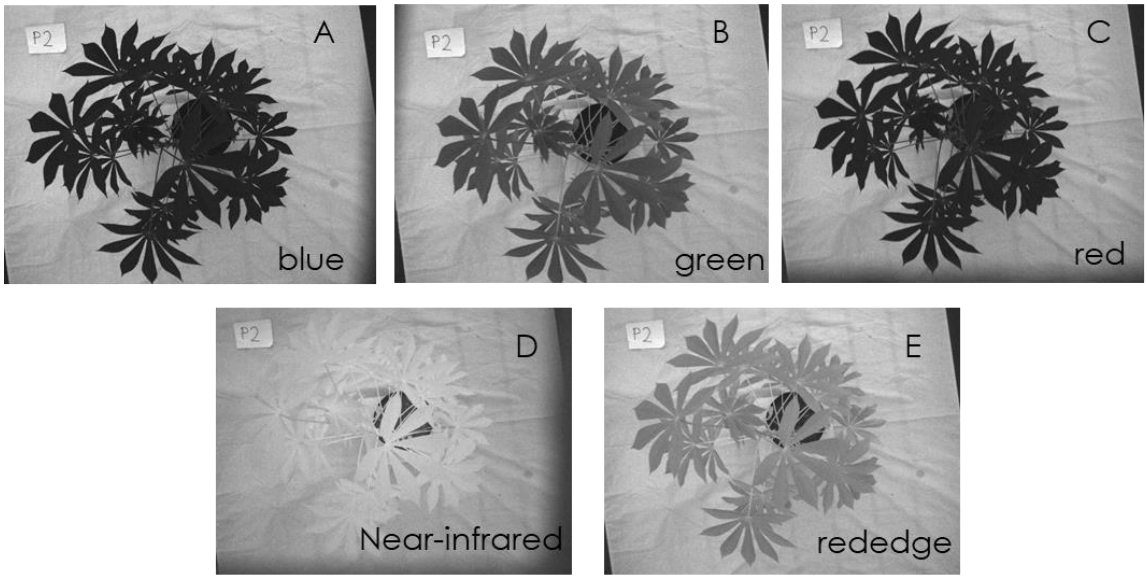

Figure 6. A batch of multispectral images of one plant in their separate bands (blue, green, red, near-infrared, and red edge).

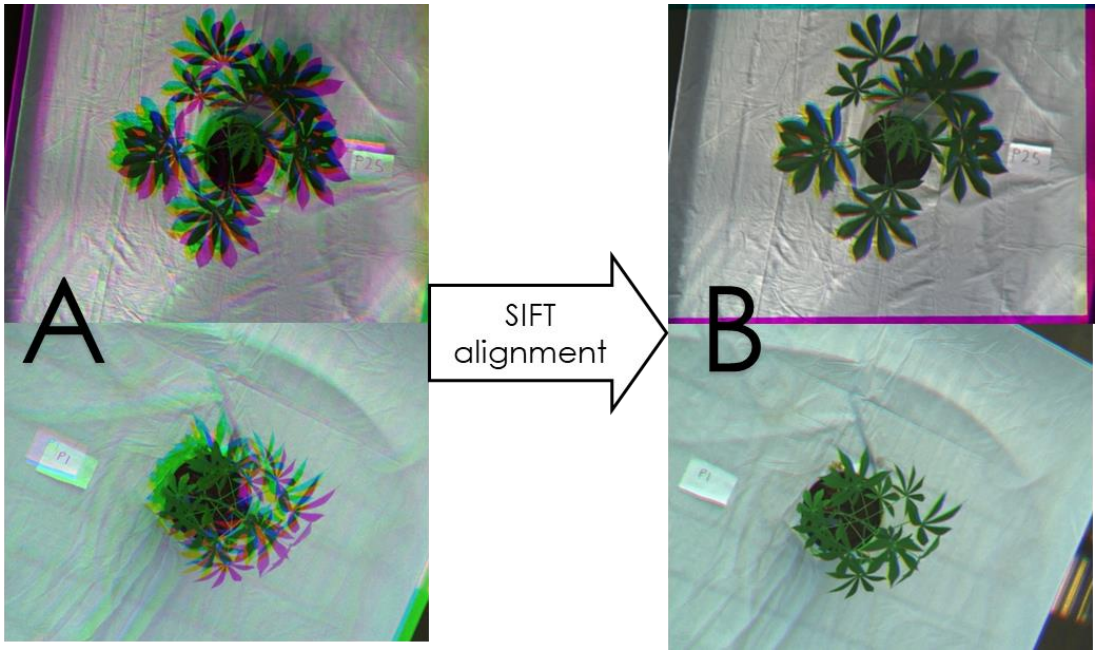

Figure 7. Shows before and after aligning the images with the SIFT algorithm. Initially, when the images in the various band were stacked on each other to perform the NDVI analysis, they were misaligned because the multispectral camera sensors are not coaxial. But after processing the images with the SIFT algorithm, they aligned quite well.

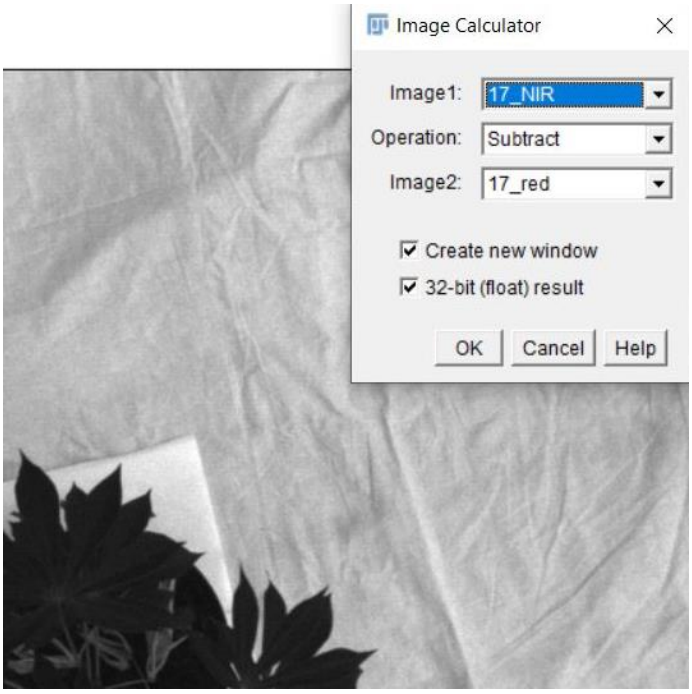

Figure 8. Screenshot of NDVI calculation with image calculator in Fiji Image J. The image calculator is about to do only one operation at a time, hence the difference between the digital number values of near-infrared and red was computed, then their sum, and finally the former was divided by the latter.

Figure 9. Selection of plant area using a threshold after NDVI calculation. The red portion shows the area which was detected by the ImageJ as leaves using the threshold. The average digital number of the selected region was recorded as the NDVI of the plant.

4.4. Measurements and Data

The multispectral images were taken in 16-bit greyscale. With each pixel having a digital number value of 0−65535. A pixel value of 0 means all radiation in that band was absorbed and 65535 means all the radiation was reflected to the camera sensor. The multispectral image data was used for the computation of NDVI. The RGB images were captured in 24-bit color images. With each pixel having a component of red, green, and blue value. RGB images were used to compute for leaf area, GA, GGA, and CSI. Actual biomass was measured by weighing the stem, root, and leaves of the cassava plant at the end of the planting period. Chlorophyll content was measurement was done using an Apogee MC-100 meter (Apogee Instruments, Logan, UT, USA). The actual leaf area was measured using a portable leaf area meter (LI-3000; LI-COR, Lincoln, NE, USA).

4.5. Statistical analysis

Image data collected from the four experiments were combined after subjecting to contrast analysis for experimental differences. A two-way analysis of variance (ANOVA) was performed on image parameters that had good significant correlations with the directly measured ones and where there were differences in the means were separated using Tukey test at $P< 0.05$ significance. Moreover, Pearson correlation analysis was conducted between the image-extracted data and the actual measured data to determine the relationship. Statistical analyses were performed using SPSS

version 25 (IBM Corp., Armonk, NY, USA), OriginPro version 2020. Origin Corporation, Northampton, MA, USA, and R version 4.0.2.

5. Results

5.1. Correlation of data from images with data directly measured from plants

Strong positive associations were observed between parameters determined from the image data and the actual measured data, that is, chlorophyll content (CHL), whole plant biomass (WPB), and leaf area (LA). NDVI which was obtained from the multispectral images showed significant ($p < 0.01$) positive correlations with WPB, CHL, and LA (Figure 10). Also, the computed leaf area from RGB images (LA_RGB) showed significant ($p < 0.01$) correlations with WPB, CHL, and LA (Figure 11). In contrast, Crop Senescence Index (CSI) showed negative correlations with all the directly measured parameters (Figure 12). Nonetheless, the green area (GA) and greener area (GGA) which were used to compute for CSI all showed good correlations with the growth parameters (Figure 13). Other color components like hue, saturation, and intensity showed no significant correlation with any of the measured parameters.

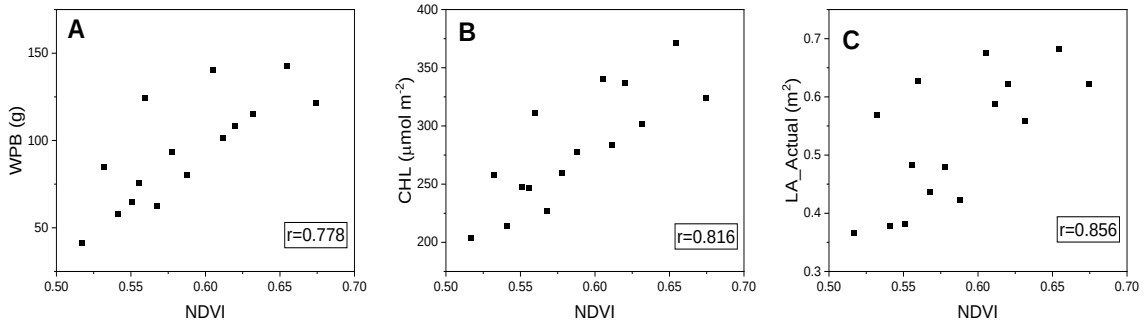

Figure 10. Scatter diagram of the means of all treatments for NDVI against whole plant biomass *p=0.001* (A), chlorophyll content *p<0.001(*B), and measured leaf area *p=0.005* (C) of young cassava plants grown under deficit irrigation and potassium fertigation. The data from four separate experiments were combined and shown as means ± SE; n = 4 to 16 replicate plants. r = correlation coefficient.

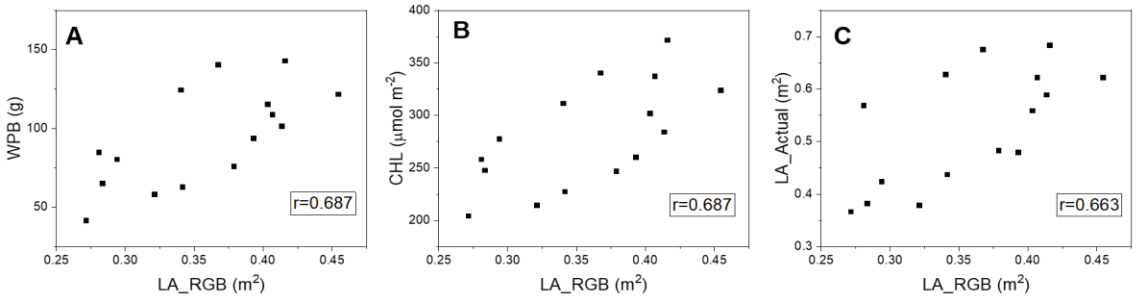

Figure 11. Scatter diagram of the means of all treatments for RGB image leaf area against whole plant biomass *p=0.005* (A), chlorophyll content *p=0.008* (B), and measured leaf area *p=0.007* (C). The data from four separate experiments were combined and shown as means ± SE; n = 4 to 16 replicate plants. r = correlation coefficient.

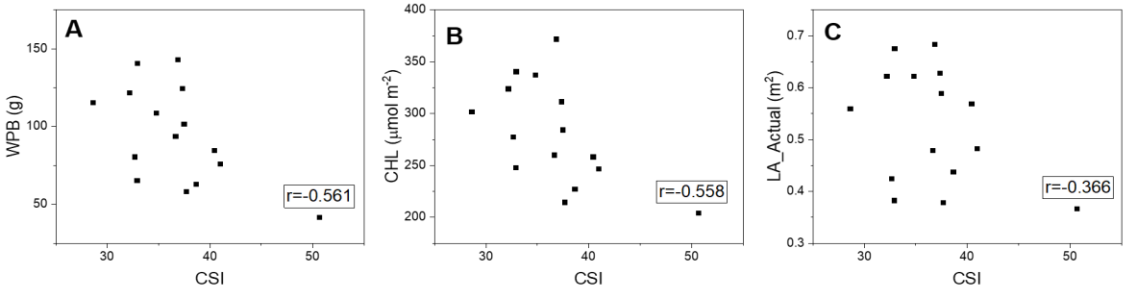

Figure 12. Scatter diagram of the means of all treatments for crop senescence index (CSI) against whole plant biomass *p=0.030* (A), chlorophyll content *p=0.031* (B), and directly measured leaf area *p=0.179* (C). CSI did not show any correlation with any of the directly measured parameters. The data from four separate experiments were combined and shown as means ± SE; n = 4 to 16 replicate plants. r = correlation coefficient

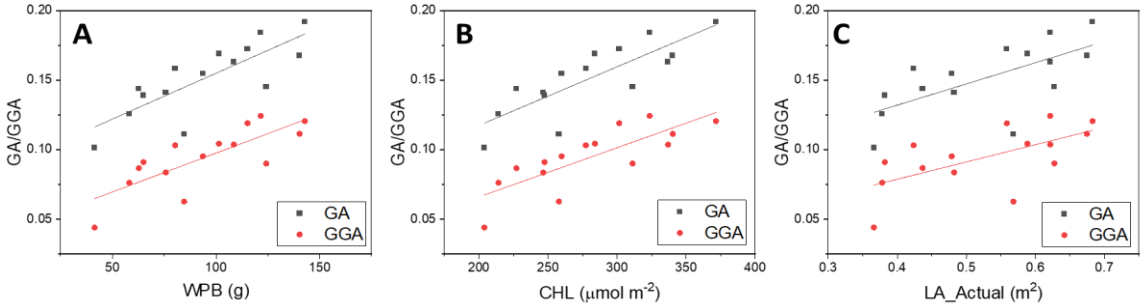

	GA	GGA	GA	GGA	GA	GGA
r	0.800	0.798	0.823	0.798	0.665	0.625
p	0.000	0.001	0.000	0.000	0.007	0.013

Figure 13. Scatter diagram of the means of all treatments for GA and GGA against whole plant biomass (A), chlorophyll content (B), and actual measured leaf area (C). Both GA and GGA showed positive correlations with the directly measured parameter. A line of best fit through GA and GGA was almost parallel to each other. The data from four separate experiments were combined and shown as means ± SE; n = 4 to 16 replicate plants.

5.2. Comparison of means

A plot of the leaf area data from the images showed that RGB imaging was able to detect the leaf area increases throughout the course of the experiment (Figure 14).

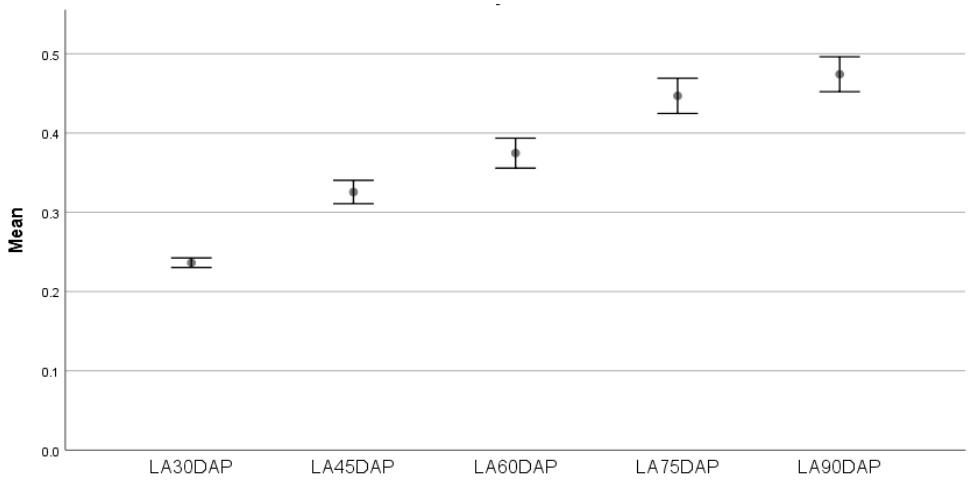

Figure 14. Mean leaf areas obtained from all the RGB images at 30, 45, 60, 75, and 90 DAP. The data from four separate experiments were combined and shown as means ± SE; n = 4 to 16 replicate plants.

A comparison of means analysis that of the leaf area computed from the images with respect to the watering and potassium treatments showed that with exception of 30 DAP, when treatment was begun, all the other days showed significant differences in means (Table 6). For watering the images observed that 60% and 100% watering levels were usually close to each other but were significantly different from 30% watering level. The image data was able to show that the different levels of potassium treatments were all mostly different from each other. For CSI, significant differences in means were only observed on the last day of data capturing (Table 7).

Table 6. ANOVA results showing the differences in the means of image leaf area by the watering and potassium treatment

Treatment			Image Leaf Area (m^2)				
			30 DAP	45 DAP	60 DAP	75 DAP	90 DAP
Watering		30%	0.23	0.29	0.32	0.36	0.40
		60%	0.23	0.31	0.38	0.43	0.49
		100%	0.23	0.32	0.38	0.46	0.54
		S.E.M	0.001	0.005	0.006	0.006	0.006
Potassium		0.01 mM	0.23	0.25	0.27	0.31	0.35
		1 mM	0.23	0.29	0.33	0.38	0.43
		4 mM	0.23	0.33	0.38	0.44	0.50
		16 mM	0.23	0.33	0.40	0.49	0.56
		32 mM	0.23	0.34	0.42	0.48	0.54
		S.E.M	0.001	0.007	0.008	0.008	0.008
Watering x Potassium	30%	0.01 mM	0.23	0.25	0.26	0.29	0.33
		1 mM	0.23	0.25	0.28	0.31	0.34
		4 mM	0.23	0.30	0.33	0.36	0.39
		16 mM	0.23	0.33	0.39	0.45	0.51
		32 mM	0.23	0.31	0.35	0.39	0.43
	60%	0.01 mM	0.23	0.25	0.28	0.31	0.34
		1 mM	0.23	0.30	0.35	0.39	0.43
		4 mM	0.23	0.36	0.39	0.46	0.53
		16 mM	0.23	0.32	0.43	0.50	0.57
		32 mM	0.23	0.32	0.45	0.51	0.56
	100%	0.01 mM	0.23	0.25	0.28	0.33	0.39
		1 mM	0.23	0.31	0.36	0.43	0.51
		4 mM	0.23	0.32	0.42	0.49	0.57
		16 mM	0.23	0.34	0.38	0.51	0.61
		32 mM	0.23	0.40	0.47	0.55	0.62
		S.E.M.	0.002	0.012	0.014	0.014	0.014
P-values		Watering	0.986	<0.001	<0.001	<0.001	<0.001
		Potassium	1.000	<0.001	<0.001	<0.001	<0.001
		Watering x Potassium	1.000	<0.001	0.001	0.001	<0.001

Table 7. ANOVA results showing the differences in the means CSI by the watering and potassium treatment

Treatment			CSI				
			30 DAP	45 DAP	60 DAP	75 DAP	90 DAP
Watering		30%	40.7	41.9	43.3	38.9	43.7
		60%	39.8	27.3	35.6	37.9	39.1
		100%	39.1	18.8	33.0	35.9	36.6
		S.E.M	2.88	3.84	2.77	3.87	1.45
Potassium		0.01 mM	39.9	29.8	36.3	39.9	48.1
		1 mM	39.3	29.4	38.6	37.7	39.8
		4 mM	39.1	22.8	34.4	37.9	37.8
		16 mM	40.8	34.7	39.3	36.7	36.6
		32 mM	40.2	29.9	37.8	35.6	36.8
		S.E.M	3.72	4.96	3.58	4.99	1.88
Watering x Potassium	30%	0.01 mM	42.6	49.5	48.8	46.5	66.1
		1 mM	37.3	39.9	43.4	37.0	44.8
		4 mM	39.7	28.7	41.3	39.7	39.1
		16 mM	42.6	48.2	44.4	35.7	34.2
		32 mM	41.4	43.2	38.8	35.4	34.5
	60%	0.01 mM	37.0	26.4	26.0	35.1	40.3
		1 mM	42.8	27.1	39.1	40.1	38.4
		4 mM	39.1	27.4	38.3	39.5	39.9
		16 mM	41.2	24.9	34.9	37.0	36.9
		32 mM	38.7	30.8	39.6	37.8	39.8
	100%	0.01 mM	40.0	13.4	34.2	38.0	37.9
		1 mM	37.9	21.4	33.2	36.2	36.2
		4 mM	38.5	12.4	23.7	34.4	34.3
		16 mM	38.7	31.2	38.6	37.4	38.7
		32 mM	40.5	15.8	35.0	33.6	36.1
		S.E.M.	6.44	8.60	6.20	8.65	3.25
P-values		Watering	0.924	<0.001	0.026	0.859	0.003
		Potassium	0.998	0.570	0.879	0.982	<0.001
		Watering x Potassium	0.998	0.827	0.557	0.997	<0.001

Irrigation and K treatments showed significant effects on NDVI, GA, GGA, and leaf area. Notably, the interaction effect was most evident at 90 DAP.

Analysis of the variances in the means of the effects of the various treatment showed differences in the following parameters: NDVI (Figure 15), Green area (Figure 16), Greener Area (Figure 17), and Image Leaf Area (Figure 20). Differences were observed in the potassium treatment and watering treatment.

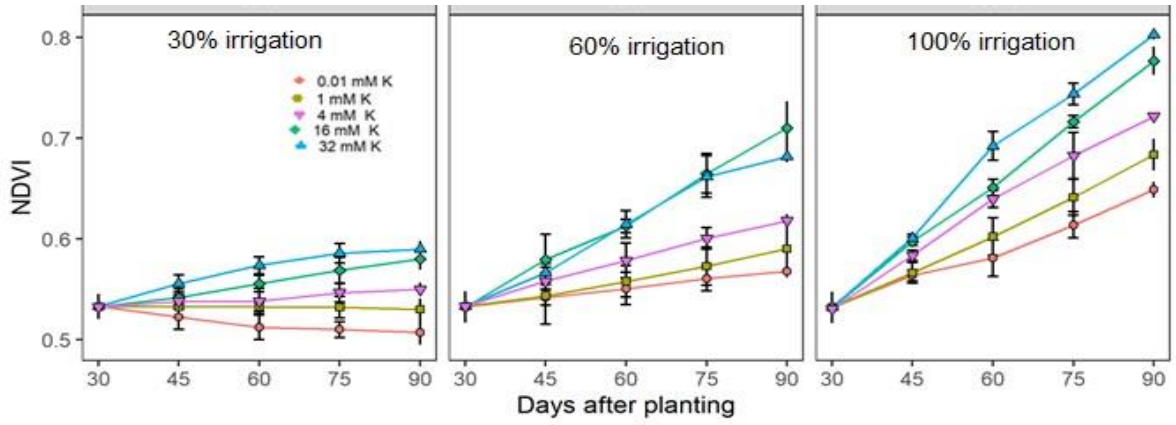

Figure 15. Comparison of means for NDVI. The data from four separate experiments were combined and shown as means ± SE; n = 4 to 16 replicate plants. $p<0.05$

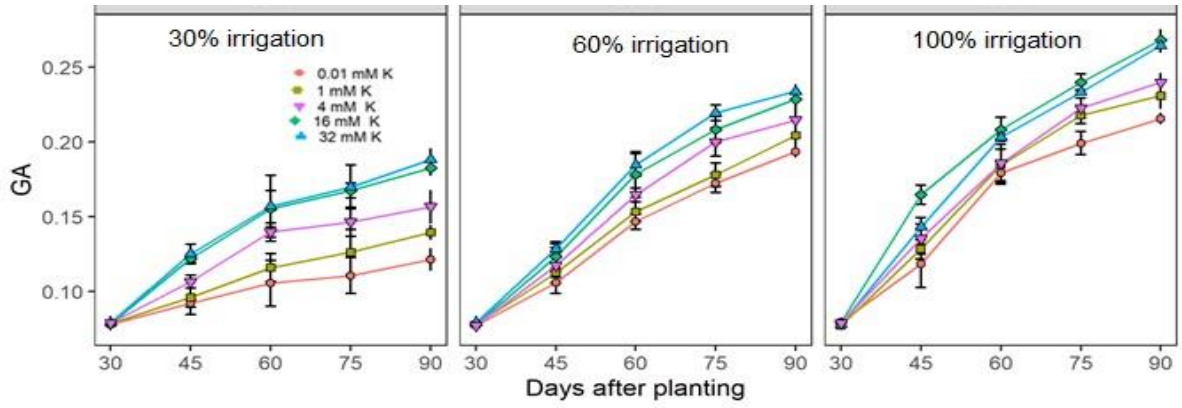

Figure 16. Comparison of means for Green Area (GA). The data from four separate experiments were combined and shown as means ± SE; n = 4 to 16 replicate plants. $p<0.05$

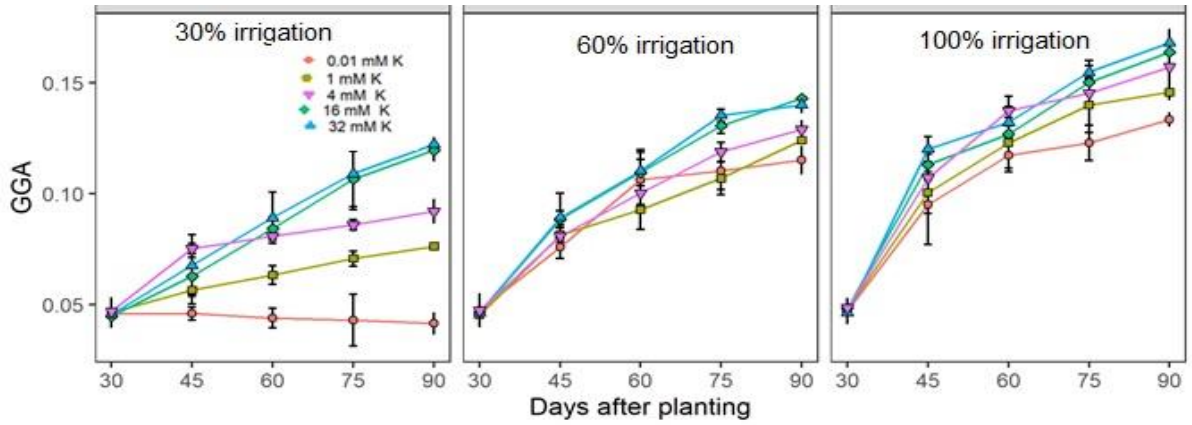

Figure 17. Comparison of means for the greener area (GGA). The data from four separate experiments were combined and shown as means ± SE; n = 4 to 16 replicate plants. $p<0.05$

6. Discussion

This study investigated the potential use of RGB and multispectral images in predicting the growth performance of young cassava grown under deficit watering and K fertigation in a greenhouse. As at the time of conducting this study not much of such study has been conducted.

6.1. Leaf area

The results show that the leaf area computed from the RGB images had a good correlation with the directly measured with a correlation coefficient greater than 0.6 (Kirk et al. 2009). It was however less than 0.8 which meant it was not a very strong correlation. This could be due to factors that affected the leaves that could be captured in the images like the color of leaves, and orientation of leaves relative to the camera (Hosoi 2007) During some of the image capturing days, some plants had yellow or dead ones which were brown. These leaves could not be identified as leaves by the threshold set by Easy Leaf Area software as seen in Figure 23 (A). Also, because the images were taken while the plants were still young, more portions of the stems and petioles were still green and hence were identified by the software as leaves like the portion denoted as B in Figure 19.

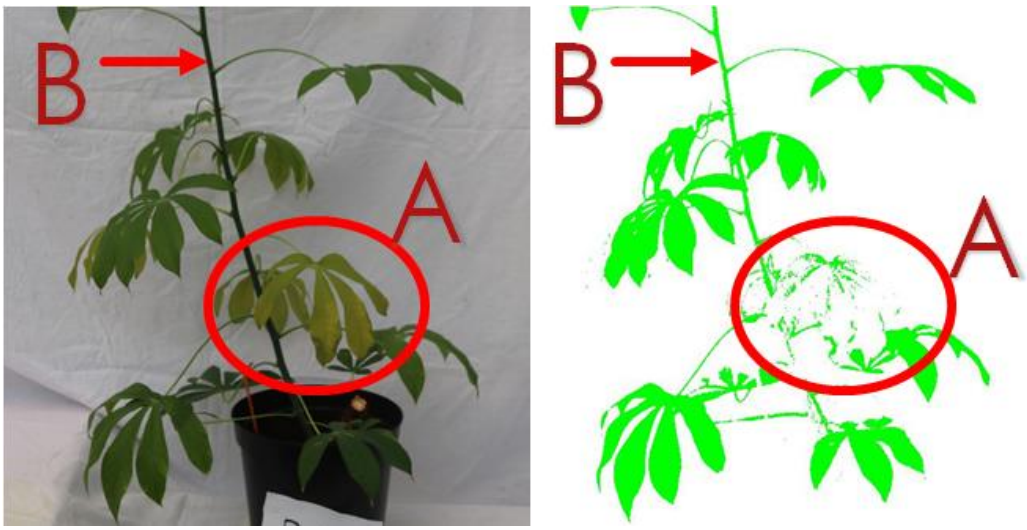

Figure 19. Comparison of between an RGB image of cassava leaves and an image of the green areas that were identified by Easy Leaf Area software. It was observed that yellow leaves could not be captured by the green threshold (A). Also, other parts of the plant, other than leaves, that were green enough were captured by the software as leaves (B).

The leaf area extracted from the images also showed strong correlations with the measured biomass which is consistent with findings by Bartelink (1997). This was because the cassava plants with taller stems have more leaves growing on them hence a simple deduction could be made that leaf area and the biomass had a direct correlation. A similar experiment conducted on lettuce also found that non-destructive biomass estimation can be performed using digital images (Bumgarner et al. 2012). The measured chlorophyll also had a good correlation with leaf area as observed by Wasonga et al. (2020). A further ANOVA analysis showed that leaf area from RGB images can be used to identify the differences in the effects of the treatments.

6.2. NDVI

NDVI correlated well with the empirically measured parameters, that is, chlorophyll, biomass, and leaf area. Several studies confirm that there is a correlation between remotely sensed vegetation indices and green variables like chlorophyll. Holben et al. (1980) reported that green leaf area index correlates with both infrared/red ratio and NDVI. Bell et al. (2004) also found that the NDVI is highly correlated with chlorophyll yield. As technology in remote sensing improved, Le Maire et al. (2008) also affirmed that with appropriate calibration, NDVI could be used to estimate chlorophyll content with high precision. These are consistent with the correlation output obtained from this experiment. This is due to the absorption and reflectance properties of leaves (Gates, 1965).

Wasonga et al. (2020), showed that watering and potassium treatments affected the health/greenness and growth of leaves. Healthy green leaves absorb more visible light and reflect more Near Infrared (NIR) radiation that falls on it whiles unhealthy leaves reflect more radiation of visible light than healthy ones and absorb more NIR that hits it (NASA Earth observatory, 2000). From the mathematical formula to determine NDVI, (NIR – red) / (NIR + red), it means that the greater the NIR reflectance, the greater the NDVI. Similar to the outcome of this study, NDVI has been found to have a strong correlation with leaf area index and biomass of maize (*Zea mays*), soybean (*Glycine max*), and other plants like *Arctophila fulva* and *Eriophorum angustifolium* (Nguy-Robertson et al. 2012, Goswami et al. 2015). A further ANOVA analysis showed that NDVI indeed can identify the differences in the effects of the treatments.

6.3. CSI, GA, and GGA

The Crop Senescence Index (CSI) had a weak correlation with the parameters of interest. Research on CSI is sometimes split on its usefulness. For instance, Buchaillot et al. (2019) found that CSI has strong correlations with yield. On the other hand, Sancho-Adamson et al. (2019) observed that CSI was not able to be used to identify differences in compost treatment but GA and GGA were. GA and GGA had strong correlations with the directly measured properties. Even though CSI is computed from GA and GGA (equation 2), itself not having a good correlation with the measured parameter could be explained by the fact the line of best fit through the correlation diagrams of GA and GGA (Figure 15) were all almost parallel therefore the differences between them were all similar, hence no identifiable differences.

6.4. Practical Usability

Both multispectral and RGB cameras showed promising usefulness in estimating growth parameters of cassava but the former performed better than the latter. The NDVI that was computed from the multispectral images showed the best correlation with the growth parameters. Therefore, even though equipment that is needed to capture multispectral data is generally more expensive than that of RGB imaging, it is worth investing in. For instance, Iseki and Matsumoto (2019) used NDVI to create a model that predicted the shoot biomass of yam.

Nonetheless, the RGB also proved to be quite useful if further studies are done to investigate errors and improve accuracy. For leaf area estimation, a simple RGB image taken with even a smartphone can be used. For instance, a non-destructive leaf area estimation of cassava can be performed by taking a picture of the plant with a red card of known area in the image close to the plant. Another application could be that leaves that are cut could be laid on a white background without each overlaying on another with a red sheet of known area, the leaf area could be easily calculated with just a single snap.

6.5. Errors and sources of inaccuracies

Some factors caused errors affected the accuracy of the data that were collected. First among these was the misalignment of the multispectral images due to the geometry of the sensors of the multispectral camera as experienced by Cardim Ferreira Lima (2020). Even though the SIFT algorithm did a phenomenal job in aligning the images, there were still some minute portions of the images that did not align. This was because the images were taken from slightly different angles

and hence were not perfectly identical. This can be seen in Figure 7B. Also, because the images were taken in a greenhouse that had translucent walls, not all the solar radiation entered the greenhouse chambers hence reducing albedo. All the cameras, both multispectral and RGB, were passive, that is, they did not produce their own radiation (light), and hence required radiation sun to be bounced off from the plants to be captured. This means that any form of interference with the solar radiation will affect the amount that will be absorbed or reflected.

7. Conclusion

The study was set out to study the usability of imaging in measuring the growth parameters of cassava. It was found out that images can play a key role in research and measurements of vital information in cassava cultivation. Leaf area can be computed using simple RGB images. The images could be taken even with most common smartphones if there is a reference area of known area in the image. On a large scale, ariel images of large plots could be used to compute for leaf area index if a patch of known surface area is placed on the field. This can be used to make good estimations of biomass. Also, NDVI is a good indicator of growth performance in young cassava plants. It can be used to predict chlorophyll content in leaves, leaf area, and biomass. CSI on the other hand is not a very good indicator of growth performance of young cassava plants, even though GA and GGA, which were used to compute CSI, were good indicators by themselves. There were however some drawbacks that further studies should investigate. For instance, the experiment was performed in a greenhouse which has its limitations in mimicking field conditions. Further studies should therefore be done on outdoor fields to mimic real-life conditions. Also, studies involving other vegetation indexes should be done to get more knowledge in this area.

8. Acknowledgment

The author would like to thank Prof. Laura Alakukku for the supervision and guidance of this project, and to Daniel Wasonga for allowing me to be part of this research project. Thanks also go to Mirko Pavicic for the crucial technical advice. Special gratitude also goes to Eunice Attafuah for the support and encouragement.

9. Bibliography

Abràmoff, M.D., Magalhães, P.J. And Ram, S.J., 2004. Image Processing With Imagej. Biophotonics International, 11(7), Pp. 36-42.

Aggarwal, S., 2004. Principles Of Remote Sensing. Satellite Remote Sensing And Gis Applications In Agricultural Meteorology, Pp. 23-38.

Alsultanny, Y. 2010. Color image segmentation to the RGB and HSI model based on region growing algorithm.

Araus, J.L. and Kefauver, S.C., 2018. Breeding to adapt agriculture to climate change: affordable phenotyping solutions. Current Opinion in Plant Biology, 45, pp.237-247.

ARAUS, J.L., KEFAUVER, S.C., ZAMAN-ALLAH, M., OLSEN, M.S., and CAIRNS, J.E., 2018. Translating High-Throughput Phenotyping into Genetic Gain.

Bartelink, H.H., 1997. Allometric relationships for biomass and leaf area of beech (Fagus sylvatica L). In Annales des sciences forestières (Vol. 54, No. 1, pp. 39-50). EDP Sciences.

Bell, G.E., Howell, B.M., Johnson, G.V., Raun, W.R., Solie, J.B., and Stone, M.L., 2004. Optical sensing of turfgrass chlorophyll content and tissue nitrogen. HortScience, 39(5), pp.1130-1132.

Bendig, J., Bolten, A., Bennertz, S., Broscheit, J., Eichfuss, S., and Bareth, G., 2014. Estimating biomass of barley using crop surface models (CSMs) derived from UAV-based RGB imaging. Remote sensing, 6(11), pp.10395-10412.

Brocks, S. And Bareth, G., 2018. Estimating Barley Biomass With Crop Surface Models From Oblique RGB Imagery. Remote Sensing, 10(2), Pp. 268.

Buchaillot, M., Gracia-Romero, A., Vergara-Diaz, O., Zaman-Allah, M.A., Tarekegne, A., Cairns, J.E., Prasanna, B.M., Araus, J.L. And Kefauver, S.C., 2019. Evaluating Maize Genotype Performance Under Low Nitrogen Conditions Using Rgb Uav Phenotyping Techniques. Sensors, 19(8), Pp. 1815.

Bumgarner, N.R., Miller, W.S. And Kleinhenz, M.D., 2012. Digital Image Analysis To Supplement Direct Measures Of Lettuce Biomass. Horttechnology, 22(4), Pp. 547-555.

Buzzard Cameras Limited, 2018. Buzzard camera datasheet https://static1.squarespace.com/static/5282956be4b0b6e93a7872a2/t/59f9ad3c27ef2d236827b9ca/1509535039066/Camera+Datasheet+Six.pdf. Sited on July 17, 2020

Cambaza, E., Koseki, S., and Kawamura, S., 2019. Why RGB Imaging Should be Used to Analyze Fusarium Graminearum Growth and Estimate Deoxynivalenol Contamination

Cardim Ferreira Lima, M., Krus, A., Valero, C., Barrientos, A., del Cerro, J. and Roldán-Gómez, J.J., 2020. Monitoring Plant Status and Fertilization Strategy through Multispectral Images. Sensors, 20(2), p.435.

Carlson, T.N. and Ripley, D.A., 1997. On the relation between NDVI, fractional vegetation cover, and leaf area index. Remote sensing of Environment, 62(3), pp.241-252.

Carper, W., Lillesand, T., And Kiefer, R., 1990. The Use Of Intensity-Hue-Saturation Transformations For Merging Spot Panchromatic And Multispectral Image Data. Photogrammetric Engineering And Remote Sensing, 56(4), Pp. 459-467.

Casadesús, J., Kaya, Y., Bort, J., Nachit, M. M., Araus, J. L., Amor, S., et al. 2007. Using vegetation indices derived from conventional digital cameras as selection criteria for wheat breeding in water-limited environments. Ann. Appl. Biol. 150, 227–236. DOI: 10.1111/j.1744-7348.2007.00116.x

Chen, D., Shi, R., Pape, J., Neumann, K., Arend, D., Graner, A., Chen, M., and Klukas, C., 2018. Predicting Plant Biomass Accumulation From Image-Derived Parameters. Gigascience, 7(2), Pp. Giy001.

Deering, D.W., 1978. Rangeland reflectance characteristics measured by aircraft and spacecraft sensors. Ph.D. Dissertation, Texas A & M University: College Station, TX, USA; pp. 338

Dogan, A., Uyak, C., Keskin, N., Akcay, A., Sensoy, R.I.G. And Ercisli, S., 2018. Grapevine Leaf Area Measurements By Using Pixel Values. Comptes Rendus De L'académie Bulgare Des Sciences, 71(6), Pp. 772-779.

Dutta Gupta, Snehasish & Ibaraki, Yasuomi & Trivedi, Priyanka. 2014. Applications of RGB color imaging in plants. 10.1201/b17441-4.

Dyer, J., Verri, G. And Cupitt, J., 2013. Multispectral Imaging In Reflectance And Photo-Induced Luminescence Modes: A User Manual. British Museum.

Ealson HM and Bloom AJ. 2014. Easy leaf area: Automated digital image analysis for rapid and accurate measurement of leaf area. Appl. Plant Sci. 2: 1-4.

Easlon, H.M. and Bloom, A.J., 2014. Easy Leaf Area: Automated Digital Image Analysis For Rapid And Accurate Measurement Of Leaf Area. Applications In Plant Sciences, 2(7), Pp. 1400033.

Gao, S., Niu, Z., Huang, N. And Hou, X., 2013. Estimating The Leaf Area Index, Height, and Biomass Of Maize Using Hj-1 And Radarsat-2. International Journal Of Applied Earth Observation And Geoinformation, 24, Pp. 1-8.

Gates, D.M., Keegan, H.J., Schleter, J.C. and Weidner, V.R., 1965. Spectral properties of plants. Applied Optics, 4(1), pp.11-20.

Gerland, P., Raftery, A.E., Ševčíková, H., Li, N., Gu, D., Spoorenberg, T., Alkema, L., Fosdick, B.K., Chunn, J., Lalic, N. and Bay, G., 2014. World population stabilization unlikely this century. Science, 346(6206), pp.234-237.

Ghanem, M.E., Marrou, H. and Sinclair, T.R., 2015. Physiological phenotyping of plants for crop improvement. Trends in Plant Science, 20(3), pp.139-144.

Gitelson, A.A.; Viña, A.; Rundquist, D.C.; Ciganda, V.; Arkebauer, T.J., 2005**.** Remote estimation of canopy chlorophyll content in crops. *Geophys. Res. Lett*, *32*, DOI:10.1029/2005Gl022688

Gizaw SA, Garland-Campbell K and Carter AH. 2016. Use of spectral reflectance for indirect selection of yield potential and stability in Pacific Northwest winter wheat. Field Crops Res. 196: 199-206.

Goswami, S., Gamon, J., Vargas, S. And Tweedie, C., 2015. No Title. Relationships Of Ndvi, Biomass, And Leaf Area Index (Lai) For Six Key Plant Species In Barrow, Alaska.

Gracia-Romero, A., Kefauver, S.C., Vergara-Díaz, O., Zaman-Allah, M.A., Prasanna, B.M., Cairns, J.E. And Araus, J.L., 2017. Comparative Performance Of Ground Vs. Aerially Assessed Rgb And Multispectral Indices For Early-Growth Evaluation Of Maize Performance Under Phosphorus Fertilization. Frontiers In Plant Science, 8, Pp. 2004.

Holben, B.N., Tucker, C.J. and Fan, C.J., 1980. Spectral assessment of soybean leaf area and leaf biomass. Photogrammetric Engineering and Remote Sensing, 46(5), pp.651-656.

Hosoi, F. And Omasa, K., 2007. Factors Contributing To Accuracy In The Estimation Of The Woody Canopy Leaf Area Density Profile Using 3d Portable Lidar Imaging. Journal Of Experimental Botany, 58(12), Pp. 3463-3473.

Huete, A.; Didan, K.; Miura, T.; Rodriguez, E.P.; Gao, X.; Ferreira, L.G., 2002. Overview of the radiometric and biophysical performance of the MODIS vegetation indices. *Remote Sens. Environ.*, *83*,195-213

Huete, A.R. A 1988. Soil-adjusted vegetative index (SAVI). Remote Sens. Environ., 25, 295-309.

Iseki, K. and Matsumoto, R., 2019. Non-destructive shoot biomass evaluation using a handheld NDVI sensor for field-grown staking Yam (*Dioscorea rotundata Poir*.). Plant Production Science, 22(2), pp.301-310.

Jarvis, A., Ramirez-Villegas, J., Campo, B.V.H. and Navarro-Racines, C., 2012. Is cassava the answer to African climate change adaptation? Tropical Plant Biology, 5(1), pp.9-29.

Jiang, Z., Huete, A.R., Chen, J., Chen, Y., Li, J., Yan, G. And Zhang, X., 2006. Analysis Of Ndvi And Scaled Difference Vegetation Index Retrievals Of Vegetation Fraction. Remote Sensing Of Environment, 101(3), Pp. 366-378.

Jordan, C.F., 1969. Derivation of leaf area index from the quality of light on the forest floor. *Ecology 50*, 663- 666.

Keating, B.A., Herrero, M., Carberry, P.S., Gardner, J. and Cole, M.B., 2014. Food wedges: framing the global food demand and supply challenges towards 2050. Global Food Security, 3(3-4), pp.125-132.

Kefauver, S.C., Vicente, R., Vergara-Díaz, O., Fernandez-Gallego, J.A., Kerfal, S., Lopez, A., Melichar, J.P., Serret Molins, M.D. and Araus, J.L., 2017. Comparative UAV and field phenotyping to assess yield and nitrogen use efficiency in hybrid and conventional barley. Frontiers in plant science, 8, p.1733.

Kerle, N., Janssen, L.L. And Huurneman, G.C., 2004. Principles Of Remote Sensing. ITC, Educational Textbook Series, 2, Pp. 250.

Kirk, K., Andersen, H.J., Thomsen, A.G., Jørgensen, J.R. And Jørgensen, R.N., 2009. Estimation Of Leaf Area Index In Cereal Crops Using Red–Green Images. Biosystems Engineering, 104(3), Pp. 308-317.

Lancaster, P.A. and Brooks, J.E. 1983. Cassava leaves as human food. Econ. Bot. 37: 331–348

Le Maire, G., François, C., Soudani, K., Berveiller, D., Pontailler, J.Y., Bréda, N., Genet, H., Davi, H. and Dufrêne, E., 2008. Calibration and validation of hyperspectral indices for the estimation of broadleaved forest leaf chlorophyll content, leaf mass per area, leaf area index and leaf canopy biomass. Remote Sensing of Environment, 112(10), pp.3846-3864.

Lee, Y.; Yang, C.; Chang, K.; Shen, Y. A., 2008. simple spectral index using reflectance of 735 nm to assess nitrogen status of rice canopy. *Agron. J. 100*, 202-212

Li, L., Zhang, Q. And Huang, D., 2014. A Review Of Imaging Techniques For Plant Phenotyping. Sensors (Basel, Switzerland), 14(11), Pp. 20078-20111.

Lillesand, T., Kiefer, R.W. and Chipman, J., 2015. Remote sensing and image interpretation. John Wiley & Sons.

Lindeberg, T., 2012. Scale Invariant Feature Transform.

Mabrouk A. EL-Sharkawy, 2003. Cassava biology and physiology. Centro Internacional de Agricultura Tropical (CIAT), A.A. 6713, Cali, Valle, Colombia; present address: A.A.

Merzlyak, M.N.; Gitelson, A.A.; Chivkunova, O.B.; Rakitin, V.Y., 1999. Non-destructive optical detection of leaf senescence and fruit ripening. Physiol. Plant., 106, 135-141.

MicaSense Inc, 2015. MicaSense RedEdge™ 3 Multispectral Camera user manual http://www.leptron.com/manuals/RedEdge_User_Manual.pdf Sited on July 17, 2020

NASA Earth observatory. 2000. Measuring Vegetation Published https://earthobservatory.nasa.gov/features/MeasuringVegetation/measuring_vegetation_2.php Aug 30, 2000. Accessed Jul 12, 2020

Nguy-Robertson, A., Gitelson, A., Peng, Y., Viña, A., Arkebauer, T. And Rundquist, D., 2012. Green Leaf Area Index Estimation In Maize And Soybean: Combining Vegetation Indices To Achieve Maximal Sensitivity. Agronomy Journal, 104(5), Pp. 1336-1347.

Norgard, J. And Best, G.L., 2017. The Electromagnetic Spectrum. National Association Of Broadcasters Engineering Handbook.

Okogbenin E, Setter TL, Ferguson M, Mutegi R, Ceballos H, Olasanmi B and Fregene M. 2013. Phenotypic approaches to drought in cassava: Front. Physiol. 4: 93-108.

Parrot drones SAS, 2017. Parrot sequoia user manual. https://support.parrot.com/files/s3fs-public/firmware/sequoia-userguide-en-fr-es-de-it-pt-ar-zn-zh-jp-ko_0.pdf. Sited on July 17, 2020

Pullanagari, R.R., Yule, I.J., Hedley, M.J., Tuohy, M.P., Dynes, R.A. and King, W.M., 2012. Multi-spectral radiometry to estimate pasture quality components. Precision Agriculture, 13(4), pp.442-456.

Rasband, W.S., 1997. ImageJ.

Samuelsson, R., Burvall, J. and Jirjis, R., 2006. Comparison of different methods for the determination of moisture content in biomass. Biomass and Bioenergy, 30(11), pp.929-934.

Sancho-Adamson, M., Trillas, M.I., Bort, J., Fernandez-Gallego, J.A. And Romanyà, J., 2019. Use Of Rgb Vegetation Indexes In Assessing Early Effects Of Verticillium Wilt Of Olive In

Asymptomatic Plants In High And Low Fertility Scenarios. Remote Sensing, 11(6), Pp. 607.

Sentera Inc, 2017. Sentera quad field agent product datasheet. https://sentera.com/product/sentera-quad-sensor. Sited on July 17, 2020.

Smith, W. K., Schoettle, A. W., Cui, M. Importance of the method of leaf area measurement to the interpretation of gas exchange of complex shoots, Tree Physiology, Volume 8, Issue 2, March 1991, Pages 121–127,

Tetracam Inc, 2017 Product details http://www.tetracam.com/Products-ADC_Micro.htm. Sited on July 17, 2020.

United Nations, Department of Economic and Social Affairs Population Division. World Population Prospects 2019 https://population.un.org/wpp/Publications/Files/WPP2019_10KeyFindings (assessed on 02.07.2020)

Use of Calibrated Reflectance Panels For RedEdge Data. https://support.micasense.com/hc/en-us/articles/115000765514-Use-of-Calibrated-Reflectance-Panels-For-RedEdge-. Published 2019. Accessed 17.03.2020

Wasonga, D.O., Kleemola, J., Alakukku, L. and Mäkelä, P.S., 2020. Growth Response of Cassava to Deficit Irrigation and Potassium Fertigation During the Early Growth Phase. Agronomy, 10(3), p.321.

Williams Iii, L. And Martinson, T.E., 2003. Nondestructive Leaf Area Estimation Of 'Niagara'and 'Dechaunac'grapevines. Scientia Horticulturae, 98(4), Pp. 493-498.

Zaman-Allah, M., Vergara, O., Araus, J. L., Tarekegne, A., Magorokosho, C., Zarco-Tejada, P. J. et al. (2015). Unmanned aerial platform-based multispectral imaging for field phenotyping of maize. Plant Methods 11:35. DOI: 10.1186/s13007-015-0078-2